J. Fluid Mech. (1965), *vol.* 21, *part* 4, *pp.* 623–633
Printed in Great Britain

Numerical solutions for the time-dependent viscous flow between two rotating coaxial disks

By CARL E. PEARSON
Sperry Rand Research Center, Sudbury, Massachusetts

(Received 21 July 1964)

The nature of the steady-state viscous flow between two large rotating disks has often been discussed, usually qualitatively, in the literature. Using a version of the numerical method described in the preceding paper (Pearson 1965), digital computer solutions for the time-dependent case are obtained (steady-state solutions are then obtainable as limiting cases for large times). Solutions are given for impulsively started disks, and for counter-rotating disks. Of interest is the fact that, at high Reynolds numbers, the solution for the latter problem is unsymmetrical; moreover, the main body of the fluid rotates at a higher angular velocity than that of either disk.

1. Introduction

By assuming the axial velocity to be radius-independent, Kármán (1921) obtained a set of ordinary differential equations describing the steady-state viscous flow above an infinitely large rotating disk; numerical solutions of these equations have been given by Cochran (1934). This problem is of considerable interest, since it provides one of the few cases in which exact solutions of the Navier–Stokes equations are feasible. Batchelor (1951) has generalized the Kármán method to the case of two rotating disks, and has discussed semi-quantitatively the nature of the steady flow between the two disks. Further comments have been made by Stewartson (1953). In some cases, such as that in which the two disks rotate in opposite directions, there has been some question in the literature as to the character of the flow.

A time-dependent disk problem has been considered by Greenspan & Howard (1963); by linearizing the equations of motion, they were able to analyse the case in which the two disks, rotating in unison, have their common angular velocity impulsively altered by a small amount. They found that the state of rigid rotation was restored in a dimensionless time of order $R^{\frac{1}{2}}$ (where R is the Reynolds number $\Omega L^2/\nu$), which represents the build-up time for an Ekman boundary layer; superimposed on this decaying normal mode are a number of decaying oscillatory modes which oscillate with twice the frequency of rotation. More recent work by Greenspan & Weinbaum (1964) extends the analysis to include higher-order terms in this 'spin-up' problem. Another linearized time-dependent disk problem, in which a single disk oscillates with a frequency ω about a steady rotation velocity Ω, has been analysed by Benney (1964). For $\omega \simeq 2\Omega$, a resonance phenomenon involving large normal velocities can be produced.

In the present paper, we describe a method for obtaining exact numerical solutions for the flow between two infinite rotating disks, when each of the disks is given an arbitrary time-dependent rotational velocity. As we will see in § 2, solutions for the time-dependent case can be obtained by assuming the same kind of radius-dependence used by Kármán and Batchelor for the time-independent case; the result is a set of partial differential equations in one space variable and in time. These equations may be solved numerically, in a way very similar to that described for the general two-dimensional problem in the preceding paper. The numerical results can be checked by re-calculating with different mesh spacings, and also by comparison with analytical solutions (such as that for the initial motion in a spin-up problem) available for special cases.

Results are presented for cases in which (*a*) one disk is held fixed, and the other disk is impulsively started from rest, (*b*) both disks are impulsively started from rest in opposite directions, with the same angular velocity, and (*c*) both disks are impulsively started from rest in opposite directions, with different angular velocities. Results for the case in which the common angular velocity of the two disks is impulsively altered from some initial value are given in Greenspan & Weinbaum (1964). Steady-state solutions for a variety of rotating disk problems are obtained from these time-dependent solutions by simply allowing the new disk velocities to persist for a very long time. As might be expected, the value of the Reynolds numbers has a strong influence on the character of these various solutions. Of particular interest is the fact that at higher Reynolds numbers, there is no stable symmetrical flow between two counter-rotating disks; however, an unsymmetrical flow, in which the main body of the fluid is rotating with one of the disks (but at a higher angular velocity than that disk), is possible. (It is not known whether such a flow would be unstable with respect to three-dimensional disturbances.) Both in this case, and in that in which only one disk rotates, there can be a number of cells of inflow and outflow.

2. Equations of motion

We consider the axisymmetric time-dependent incompressible viscous flow between two infinite rotating disks. The lower disk occupies the plane $z = 0$ of figure 1, and the upper disk is placed with its plane parallel to the plane $z = 0$, and a distance L above it. Both disks are allowed to rotate about the z-axis, with angular velocities $\Omega_1(t)$ and $\Omega_2(t)$ (lower and upper disks, respectively), which are arbitrarily prescribed functions of time t. As indicated in figure 1, the co-ordinates of any point are specified by (r, θ, z), and the corresponding fluid velocities are denoted by (u, v, w). All velocities are measured with respect to an inertial system at rest. The condition of incompressibility requires that

$$(ru)_r + (rw)_z = 0, \tag{1}$$

and the Navier–Stokes equations reduce to

$$u_t + u_r u - v^2/r + u_z w = -\rho^{-1} p_r + \nu(u_{rr} + u_r/r + u_{zz} - u/r^2), \tag{2}$$

$$v_t + v_r u + uv/r + v_z w = \nu(v_{rr} + v_r/r + v_{zz} - v/r^2), \tag{3}$$

$$w_t + w_r u + w_z w = -\rho^{-1} p_z + \nu(w_{rr} + w_r/r + w_{zz}), \tag{4}$$

where p is pressure, ρ is density, ν is kinematic viscosity, and subscripts indicate partial differentiation. We introduce dimensionless variables, indicated by u^*, for example, via $r = r^*L, z = z^*L, t = t^*/\Omega_0, u = u^*L\Omega_0, v = v^*L\Omega_0, w = w^*L\Omega_0$, $p/\rho = (p/\rho)^*L^2\Omega_0^2$, $\Omega_1 = \Omega_1^*\Omega_0$, $\Omega_2 = \Omega_2^*\Omega_0$, where Ω_0 is a chosen reference value of angular velocity. The resulting equations for the dimensionless variables are identical with equations (1) through (4), except that ν is replaced by $1/R$, where the Reynolds number R is equal to $L^2\Omega_0/\nu$. We will assume this replacement to have been made, and will drop the asterisks, so that—with ν replaced by $1/R$—equations (1) through (4) are now in dimensionless form.

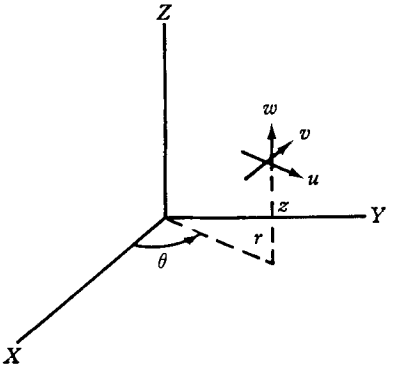

FIGURE 1. Co-ordinate system.

We look for solutions satisfying

$$w = H(z,t). \tag{5}$$

Substitution of (5) into (1) shows that

$$u = -\tfrac{1}{2}rH_z(z,t). \tag{6}$$

From (4), it now follows that $p_{zr} = 0$, so that p_r must be a function of r and t alone; thus $p_r = \phi(r,t)$. Substitution into (2) now shows that $v^2/r^2 - \phi(r,t)/r\rho$ is a function of (z,t) alone, say $G_1(z,t)$. For $z = 0$, this result requires

$$\Omega_1^2(t) - \phi(r,t)/r\rho = G_1(0,t),$$

so that ϕ/r must be independent of r. Denoting $\Omega_1^2(t) - G_1(0,t) + G_1(z,t)$ by $G(z,t)$, the result is therefore that

$$v = rG(z,t). \tag{7}$$

Differentiation of (2) with respect to z yields

$$H_{zzt} = R^{-1}H_{zzzz} - HH_{zzz} - 4GG_z, \tag{8}$$

and substitution for u, v, and w in (3) gives

$$G_t = R^{-1}G_{zz} + GH_z - G_zH. \tag{9}$$

If we can find functions $G(z,t)$ and $H(z,t)$, satisfying (8) and (9), and the boundary conditions

$$\left.\begin{aligned} G(0,t) &= \Omega_1(t), & G(1,t) &= \Omega_2(t), \\ H(0,t) &= 0, & H(1,t) &= 0, \\ H_z(0,t) &= 0, & H_z(1,t) &= 0, \end{aligned}\right\} \tag{10}$$

then equations (1) through (4), and the boundary conditions for no-slip viscous flow, will all be satisfied.

The method of numerical solution of (8) and (9) is analogous to that used in the two-dimensional problem described in the preceding paper (Pearson 1965). Equation (8) is replaced by the coupled pair of equations

$$M_t = R^{-1}M_{zz} - HM_z - 4GG_z, \tag{11}$$

$$H_{zz} = M \tag{12}$$

(which are clearly analogous to (5) and (6) of Pearson 1965), and (9), (11), (12) are then replaced by their finite-difference analogues, in implicit form. For each time-step, (9) and (11) are used to obtain new mesh-point values of M and G, and (12) is then used to find the new value of H. Equations (11) and (12) are hinged together on the first mesh point in from the two boundaries, a formula for H at these points which is accurate to second-order terms is used, and the correct new values of M at these points are determined iteratively (with appropriate smoothing)—all as in the preceding paper. Of course, since there is only one space variable, the implicit difference equation for (11) is in tri-diagonal form and so may be solved very simply by Gaussian elimination; relaxation is not necessary. On the other hand, we have one additional equation, (9), to be used at each time-step. Also as in the preceding paper, it turns out that for large values of R, internal as well as boundary smoothing must be used during the iteration process. With this smoothing, there appear to be no stability restrictions on the size of the time-step; moreover, the implicit forms of the difference equation approximations to (9) and (11) ensure high accuracy.

In many of the problems treated here, one or both boundary conditions were altered impulsively at $t = 0$. Under such conditions, finite-difference approximations can lead to substantial errors for the first few time steps; to minimize these errors, the first time-step was divided into a number of subintervals and appropriate pseudo boundary conditions chosen for the first few of these subintervals. A discussion of this method of handling impulsive boundary conditions is given in Pearson (1964).

3. Verification of numerical solution

Most of the results to be reported were checked by re-running the problem with different choices of space or time mesh. Comparison with the analysis of Greenspan & Howard and Greenspan & Weinbaum for the case in which two disks have their common angular velocity changed by a small amount showed good agreement between the numerical and analytical results; this comparison is discussed in detail in Greenspan & Weinbaum (1964). We describe here a different method whereby the numerical results have been checked for the initial motion regime in certain cases.

Consider the case in which the fluid is initially at rest, and in which the disk at $z = 0$ is impulsively given an angular velocity $\Omega = K$; the disk at $z = 1$ is held fixed. We can anticipate, and verify *a posteriori* (or from the numerical calcula-

tions) that the non-linear terms in (9) will be negligible during the initial stages of the motion, so that the solution of (9) will be

$$G(z,t) = K\{\operatorname{erfc}[z\sqrt{R}/2\sqrt{t}] - \operatorname{erfc}[(2-z)\sqrt{R}/2\sqrt{t}] + \operatorname{erfc}[(2+z)\sqrt{R}/2\sqrt{t}] - \operatorname{erfc}[(4-z)\sqrt{R}/2\sqrt{t}] + \ldots\}, \quad (13)$$

where

$$\operatorname{erfc}(\beta) = \frac{2}{\sqrt{\pi}}\int_{\beta}^{\infty} e^{-\xi^2}\,d\xi.$$

For small t, only the first term in (13) is important. On the other hand, although the term HH_{zzz} will be negligible for sufficiently small H, we cannot discard the term $-4GG_z$ in (8), since this term provides the driving force—without it, the boundary condition (10) would give $H = 0$. Thus we replace (8) by

$$H_{zzt} = R^{-1}H_{zzzz} - 4GG_z,$$

valid for small t. Two integrations with respect to z give

$$H_t = \frac{1}{R}H_{zz} + 2\int_z^{\infty} G^2(z,t)\,dz + \frac{z}{R}f(t) + \frac{1}{R}w(t), \quad (14)$$

where $f(t)$ and $w(t)$ are as yet undetermined functions of t. We solve (14) by taking a Laplace transform in time; before doing so, it is useful to simplify the function $K^2\{\operatorname{erfc}(z\sqrt{R}/2\sqrt{t})\}^2$ that appears under the integral sign, by approximating it by a function whose time-transform is relatively simple. Such a function is any linear combination of erfc functions; we write

$$\{\operatorname{erfc}(\beta)\}^2 \simeq 0{\cdot}4378\operatorname{erfc}(2{\cdot}223\beta) + 0{\cdot}5457\operatorname{erfc}(1{\cdot}401\beta), \quad (15)$$

which provides an excellent fit† for all positive values of β.

With this approximation, a transform of (14) may be taken, and the resulting ordinary differential equation in z may be solved subject to the boundary conditions (10) (the transforms of the functions $f(t)$ and $w(t)$ are also thereby determined). The inversion formula may next be applied, and the result for small t can be obtained by considering large values of s. Among the leading terms in the asymptotic expansion for H_z is only one which does not depend on z (the other leading terms are negligible except near $z = 0$ or $z = 1$), and this term gives

$$H_z \sim \frac{2K^2}{\sqrt{R}}\left\{\frac{t^{\frac{3}{2}}}{\Gamma(\frac{5}{2})} + \frac{2}{\sqrt{R}}\frac{t^2}{\Gamma(3)} + \cdots\right\}\left\{\frac{0{\cdot}4378}{(2{\cdot}223)^2+(2{\cdot}223)} + \frac{0{\cdot}5457}{(1{\cdot}401)^2+(1{\cdot}401)}\right\}. \quad (16)$$

For small t, the computational results were in excellent agreement with (16). Thus the $t^{\frac{3}{2}}$ dependence was verified, the value of H_t was almost constant over the z-range (0, 1) except near the two ends, and this almost-constant value of H_z agreed with that calculated from (16). As a typical example of the numerical agreement, the value of H_z for $R = 100$, $K = 1$, $t = 0{\cdot}02$ as given by (16) is $9{\cdot}66 \times 10^{-5}$, whereas that obtained computationally (with 800 mesh points between $z = 0$ and $z = 1$, and with time steps of 0·001) was $9{\cdot}63 \times 10^{-5}$.

† The largest error is at $\beta = 0$, where the discrepancy is 0·0165 (relative to an exact value of unity). Elsewhere, the discrepancy is much smaller. Equation (15) was obtained by allowing the computer to carry out a search process for the coefficients on the right-hand side, with the object of minimizing the mean-square discrepancy between the two sides.

4. Numerical results

Figures 2, 3, and 4 give profiles at various times for G, H, H_z, respectively, for the case in which one disk is impulsively given unit angular velocity at $t = 0$. Thus the fluid is at rest for $t < 0$; for $t > 0$, we have $\Omega_1 = 1$, $\Omega_2 = 0$. The value of R is 100. The appropriate value of t is marked on each profile. The dotted curves represent the Kármán–Cochran steady-state solution for the single-disk case.

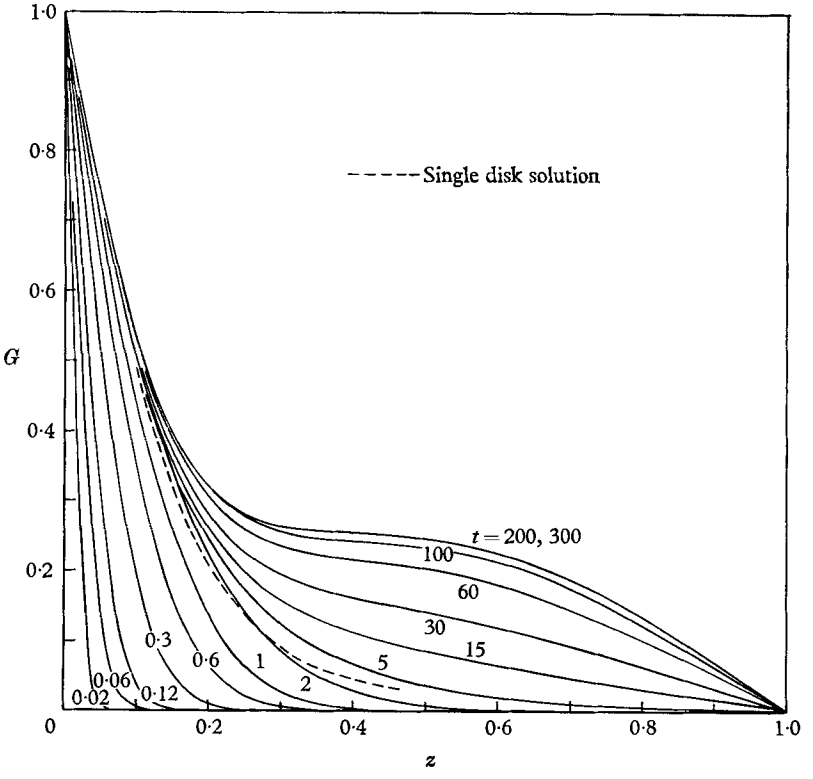

FIGURE 2. G-profiles for various values of t. $R = 100$. Left-hand disk impulsively started with $\Omega = 1$.

Figures 5, 6, and 7 give the corresponding results for $R = 1000$. Attention may be directed towards the different time regimes during the build-up of the motion, and towards the circulatory cells evident in the final motion. The increased value of G near the fixed disk, for the steady-state case, represents a similar situation to that encountered in a meteorological problem by Boedewadt (1940).

Figure 8 gives the final values of G for the case of two counter-rotating disks, with $R = 100$. Here $\Omega_1 = 1$, and the various profiles correspond to $\Omega_2 = -1$, $-0{\cdot}9$, $-0{\cdot}5$, $-0{\cdot}25$, $-0{\cdot}1$, and $-0{\cdot}04$. The dotted curves are profiles for $10H$ and H_z for the case $\Omega_2 = -0{\cdot}5$. It will be observed that, except for very small Ω_2, most of the fluid (as measured axially) is rotating with the slower disk. This is perhaps not surprising, since the predominant axial motion towards the faster disk will carry the angular momentum associated with the slower disk towards the faster disk.

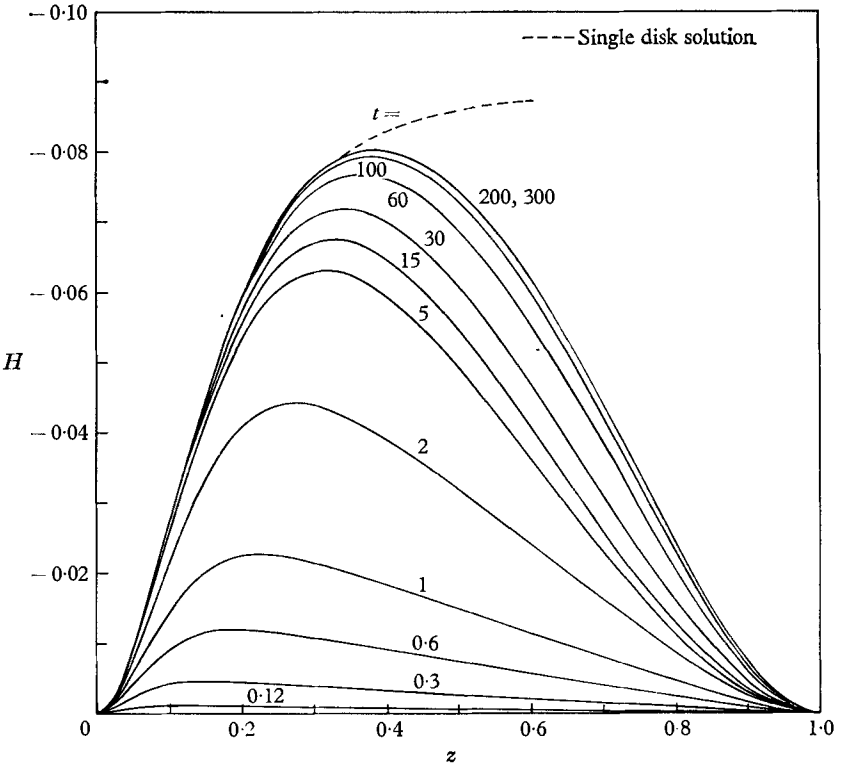

FIGURE 3. H profiles corresponding to figure 2.

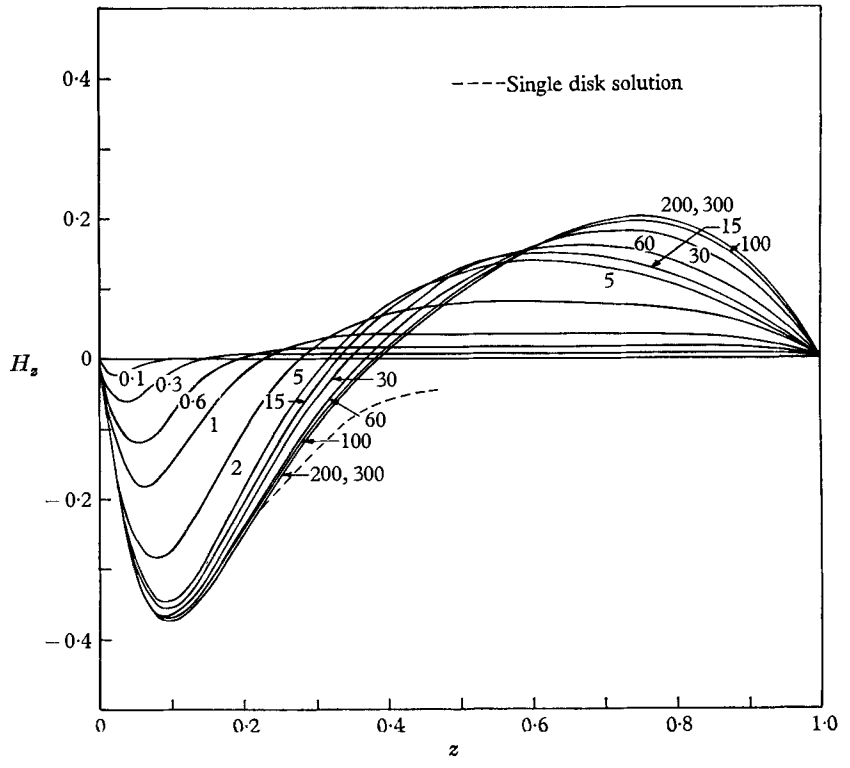

FIGURE 4. H_z profiles corresponding to figure 2.

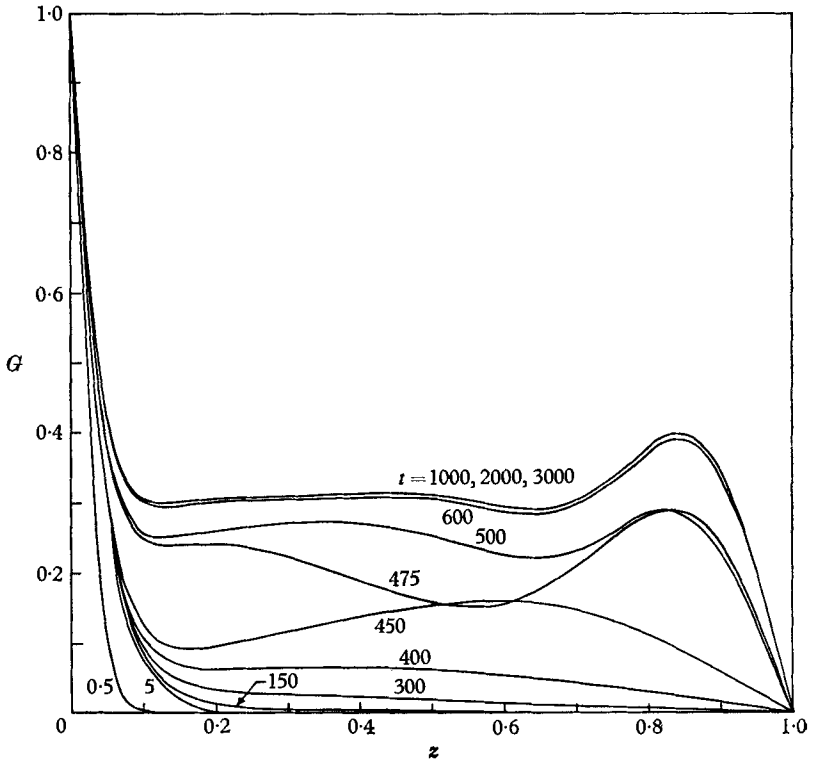

FIGURE 5. G-profiles for various values of t. $R = 1000$. Left-hand disk compulsively started with $\Omega = 1$.

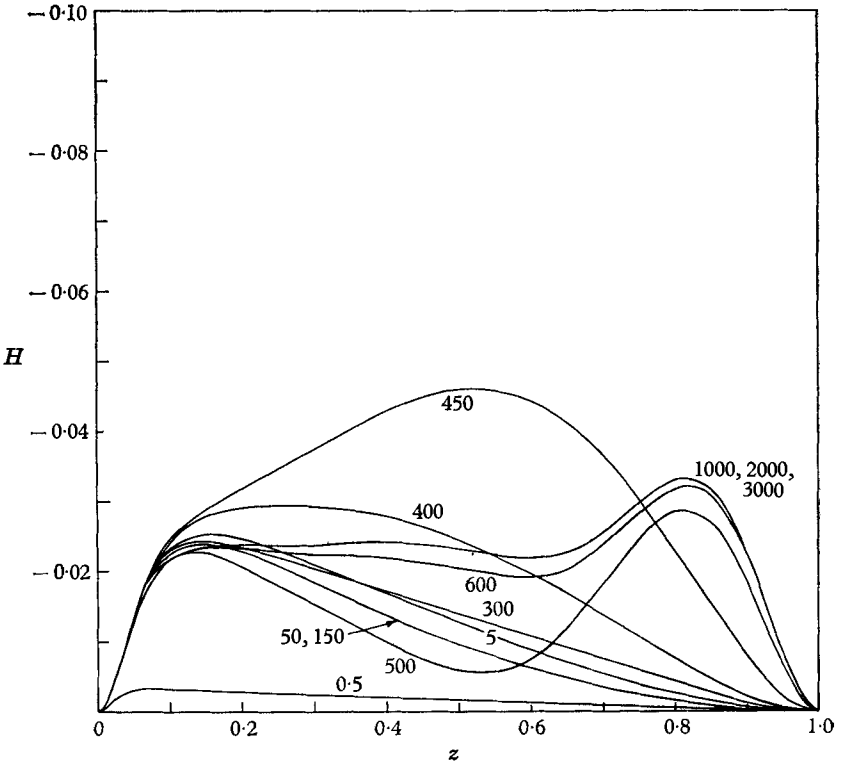

FIGURE 6. H profiles corresponding to figure 5.

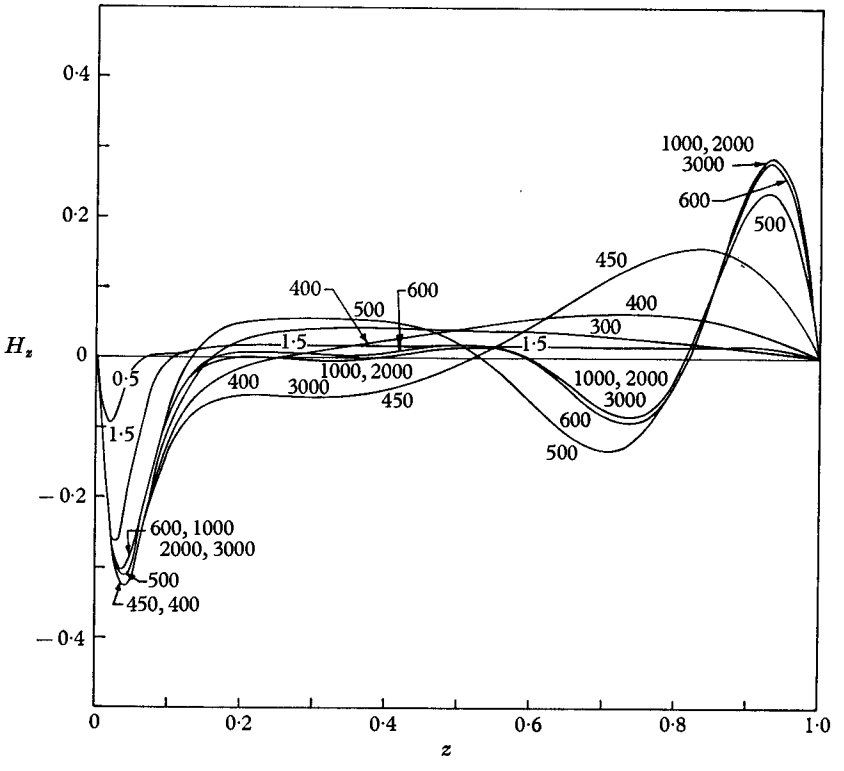

FIGURE 7. H_z profiles corresponding to figure 5.

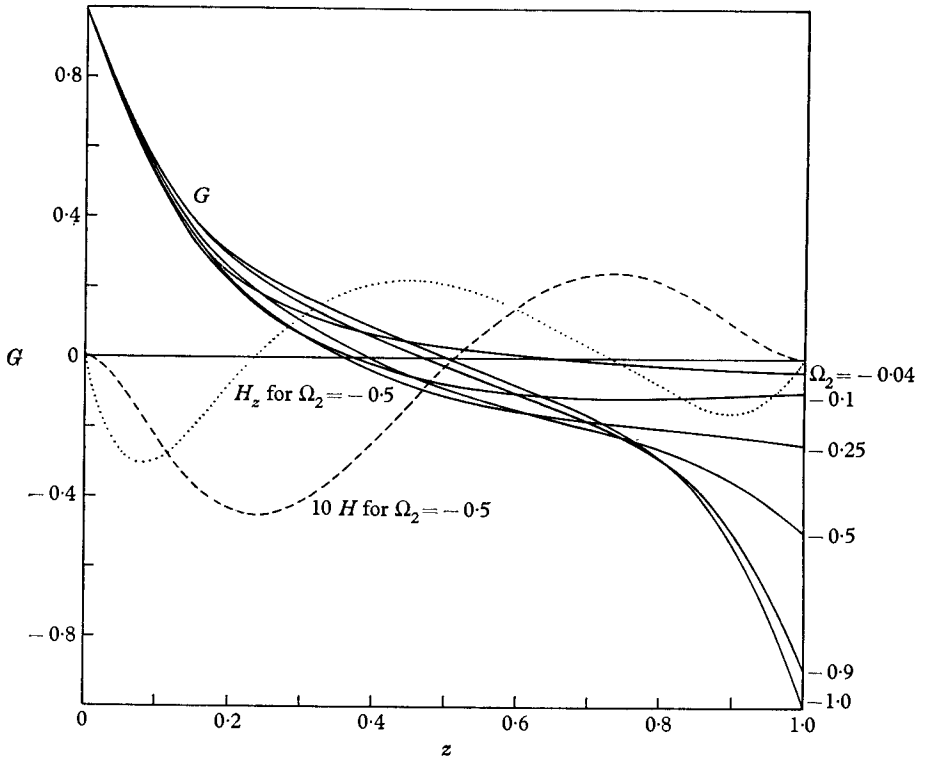

FIGURE 8. Steady-state motion for two counter-rotating disks. $R = 100$; $\Omega_1 = 1$; $\Omega_2 = -1, -0{\cdot}9, -0{\cdot}5, -0{\cdot}25, -0{\cdot}1, -0{\cdot}04$.

In figure 8, the G curve exhibits the symmetry of the motion for $\Omega_1 = 1$, $\Omega_2 = -1$. At $R = 1000$, no such symmetry was obtained; figure 9 gives curves of G, H, H_z for the steady-state motion for the case of two counter-rotating disks with $R = 1000$, $\Omega_1 = 1$, $\Omega_2 = -1$. Most of the fluid is here rotating in the same direction as the disk at $z = 0$; this is simply an accident of computer round-off early in the motion, and the opposite solution—in which most of the fluid rotates

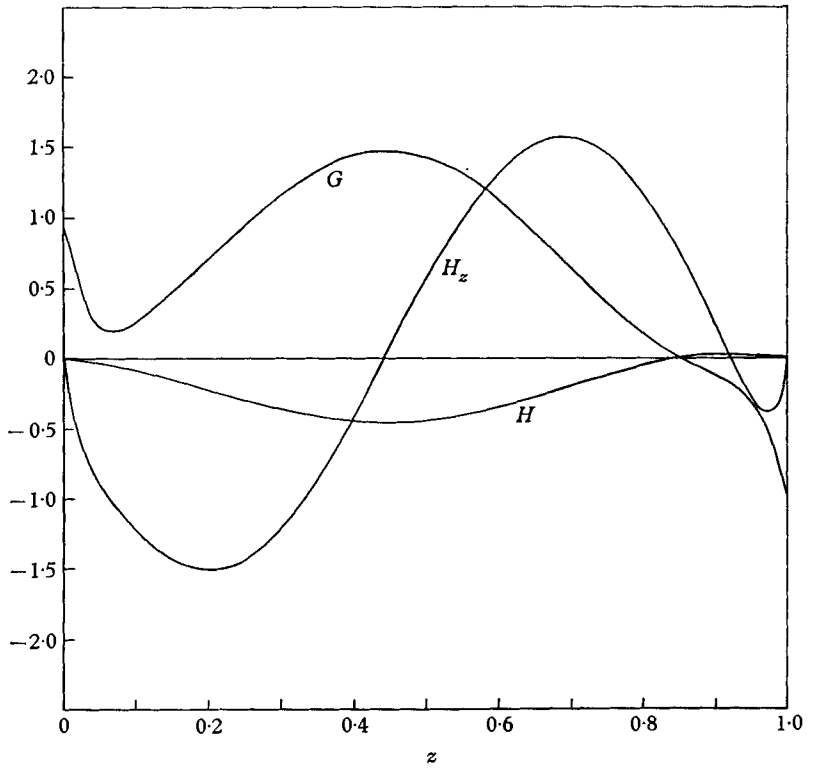

FIGURE 9. Profiles of G, H, H_z, for steady-state motion between two counter-rotating disks with $R = 1000$.

in the same direction as the disk at $z = 1$—was obtained computationally by simply starting the disk at $z = 1$ slightly before that at $z = 0$. This non-symmetrical solution starts developing at very early times; it is apparent that no symmetrical solution, stable to one-dimensional disturbances, can exist. Whether the solution given in figure 9 is stable to three-dimensional disturbances is not known. It is interesting that most of the fluid is rotating faster than either disk; physically, this is possible because of the requirement of conservation of angular momentum, as applied to initially slowly-rotating fluid migrating radially inwards, as well as towards the left-hand disk.

REFERENCES

BATCHELOR, G. K. 1951 *Quart. J. Mech. Appl. Math.* **4**, 29.
BENNEY, D. 1964 *Sperry Rand Res. Center Rep.* RR-64-6, January.
BOEDEWADT, U. T. 1940 *Z. angew. Math. Mech.* **20**, 241.
COCHRAN, W. G. 1934 *Proc. Camb. Phil. Soc.* **30**, 365.
GREENSPAN, H. P. & HOWARD, L. N. 1963 *J. Fluid Mech.* **17**, 385.
GREENSPAN, H. P. & WEINBAUM, S. 1964 *Sperry Rand Res. Center Rep.* July.
KÁRMÁN, T. V. 1921 *Z. angew. Math. Mech.* **1**, 244.
PEARSON, C. 1964 *Sperry Rand Res. Center Rep.* RR-64-29.
PEARSON, C. E. 1965 *J. Fluid Mech.* **21**, 611.
STEWARTSON, K. 1953 *Proc. Camb. Phil. Soc.* **49**, 333.